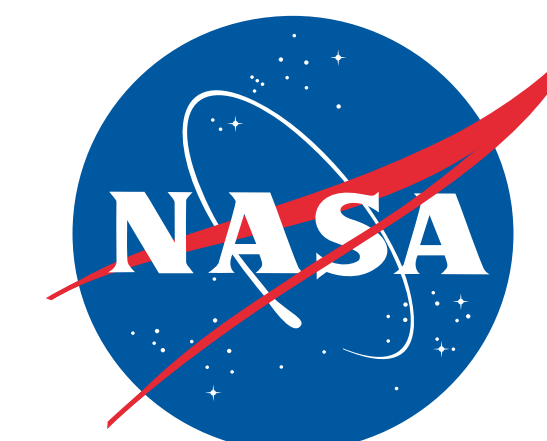


Radiometric and Polarimetric data inter-comparison for the POlarimeter DEfinition EXperiment (PODEX)

Kirk Knobelspiesse and Jens Redemann, NASA Ames Research Center, Moffett Field, California contact: kirk.knobelspiesse@nasa.gov

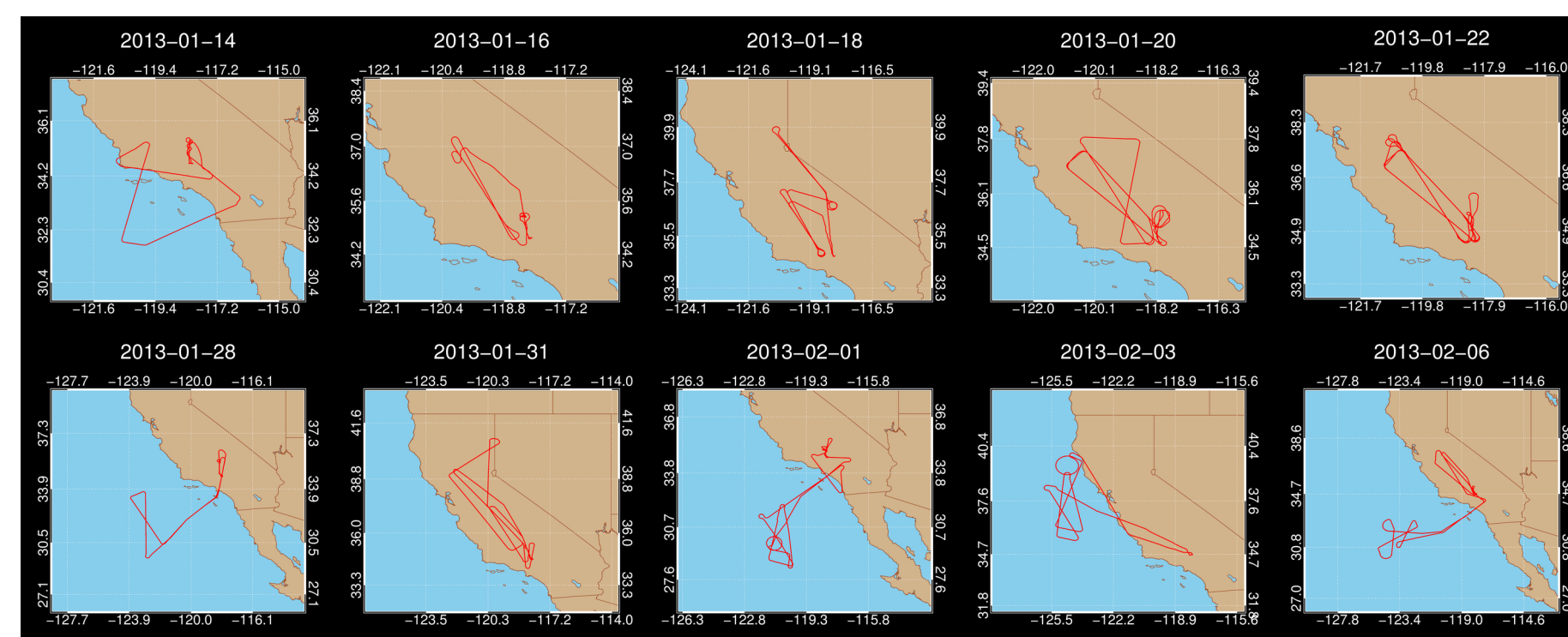


In January and February of 2013, three polarimeters were flown on the high-altitude NASA ER-2 aircraft, which was based in Palmdale, California as part of the POlarimeter DEfinition EXperiment (PODEX). The Airborne Multi-angle SpectroPolarimeter Imager (AirMSPi), Passive Aerosol and Cloud Suite (PACS) and Research Scanning Polarimeter (RSP) all employ different methods to determine polarization. Furthermore, they have a variety of spectral channels, spatial scales, measurement geometries and radiometric and polarimetric accuracies. All of these factors contribute to a sensor design's ability to determine geophysical properties of relevance to the global climate. Field deployment of airborne instruments such as AirMSPi, PACS and RSP provide valuable information for the development of future orbital instruments, such as the Aerosols-Clouds-Ecosystems (ACE) mission described by the National Research Council's Decadal Survey. For example, the complex algorithms that retrieve aerosol and cloud optical properties from polarimeters rely on realistic assessments of measurement uncertainty. We therefore compare the radiometric and polarimetric fidelity of these instruments using simultaneously observed scenes from PODEX, with the ultimate goal of improving retrieval algorithms and guiding future instrument design.

PODEX POLarimeter DEfinition EXperiment

PODEX involved ten flights of the NASA ER-2, carrying airborne prototypes of three types of optical polarimeters. Although they have variable design characteristics, these instruments are intended to determine climate relevant properties of clouds, aerosols, ocean and land surfaces. Heritage of these instruments include POLDER (CNES) and APS-Glory (which failed during launch). They are also prototypes for potential future orbital instruments such as the ACE and PACE missions of the Decadal Survey.

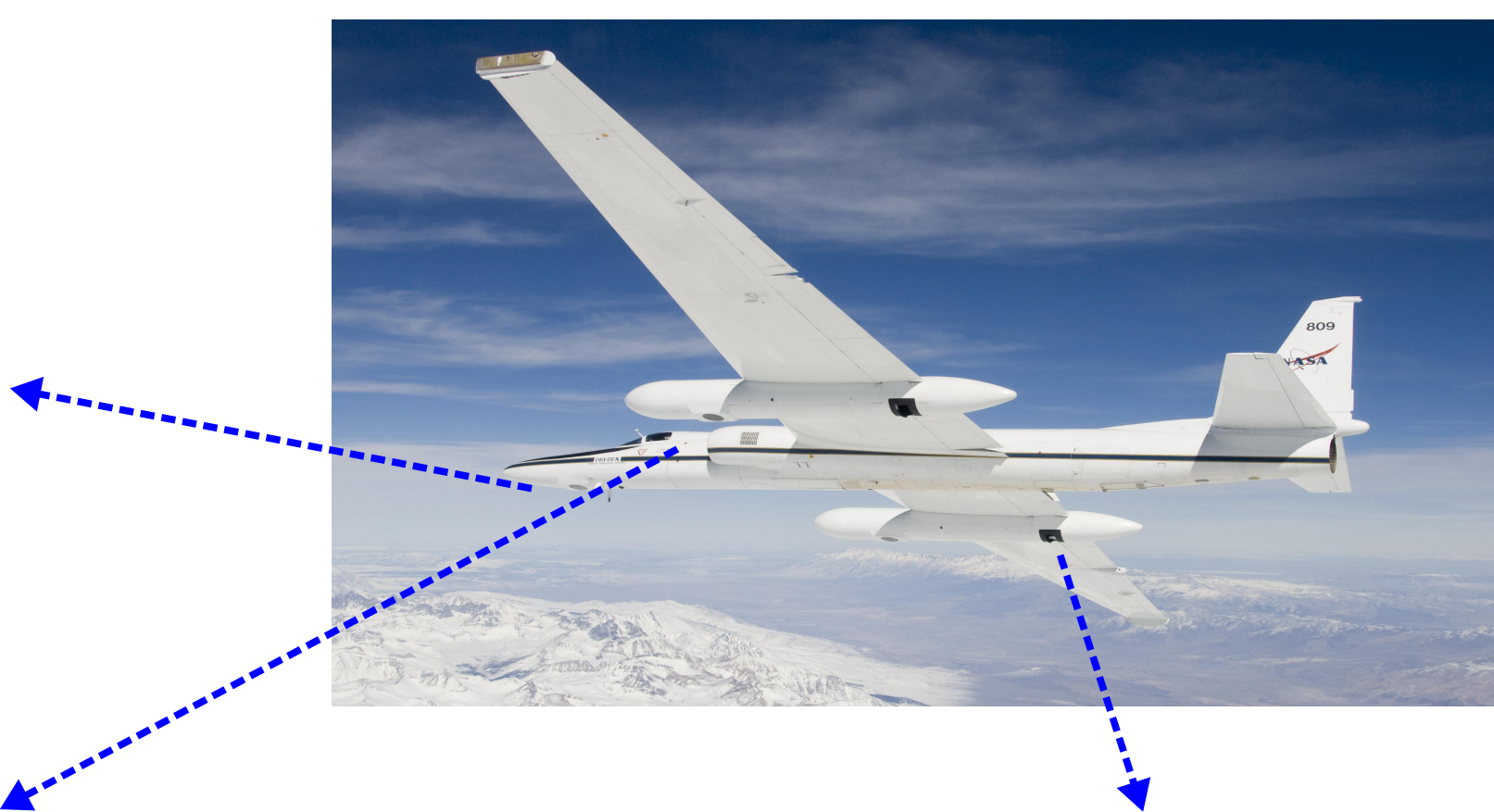
Scene Type	AirMSPi	PACS	RSP	<i>in situ</i> observations
No cloud and few aerosols over ocean	Yes	No	Yes	No
No cloud and few aerosols over land	Yes	Yes	Yes	No
Aerosol over land	Yes	Yes	Yes	Yes
Aerosol over urban surface	Yes	Yes	Yes	Yes
Aerosol over ocean	Yes	Yes	Yes	Partial
High aerosol loading	No	No	No	Yes
Broken Clouds over ocean	Yes	Yes	Yes	Yes
Tropospheric clouds	Yes	Yes	Yes	Yes
Cirrus clouds over ocean	No	No	No	No
Cirrus clouds over land	Yes	Yes	Yes	Yes
Cirrus clouds over lower clouds	Yes	Yes	Yes	Yes



PODEX was based at the NASA Dryden Aircraft Operations Facility in Palmdale, California. In addition to the three polarimeters described below, the ER-2 also flew the Autonomous Modular Sensor (AMS), Cloud Physics Lidar (CPL) and the Solar Spectral Flux Radiometer (SSFR). Flight paths are shown above. Some flights were also coordinated with aircraft from the DISCOVER-AQ field campaign. These aircraft deployed a variety of *in situ* sampling equipment. A table describing observed scenes is shown at left.

Airborne Multiangle SpectroPolarimetric Imager (AirMSPi): Pushbroom imager that uses a photoelastic modulator based technique. Principal Investigator is David J. Diner, Jet Propulsion Laboratory. See A24E-03 and A24E-04 at 4:30 and 4:45pm today, and Diner et al. (2013).

Limited dataset available:
eosweb.larc.nasa.gov/project/airmspi/airmspi_table



Passive Aerosol and Cloud Suite (PACS): Imager that uses Philips prisms to split into polarized components. Principal Investigator is J. Vanderlei Martins, University of Maryland, Baltimore County. See A24E-07 at 5:30pm today.

Data not yet available for analysis

Research Scanning Polarimeter (RSP): Scanner that uses Wollaston prisms to split into polarized components. Was the airborne prototype for the Aerosol Polarimetry Sensor on the NASA Glory Mission. Principal Investigator is Brian Cairns, NASA Goddard Institute for Space Studies. See A24E-05 and A24E-06 at 5:00 and 5:15pm today, and Cairns et al., 2003, Chowdhary et al, 2012 and Knobelspiesse et al., 2011.

Full dataset available:
www-air.larc.nasa.gov/missions/discover-aq/podex-links.html

Comparison of instrument characteristics

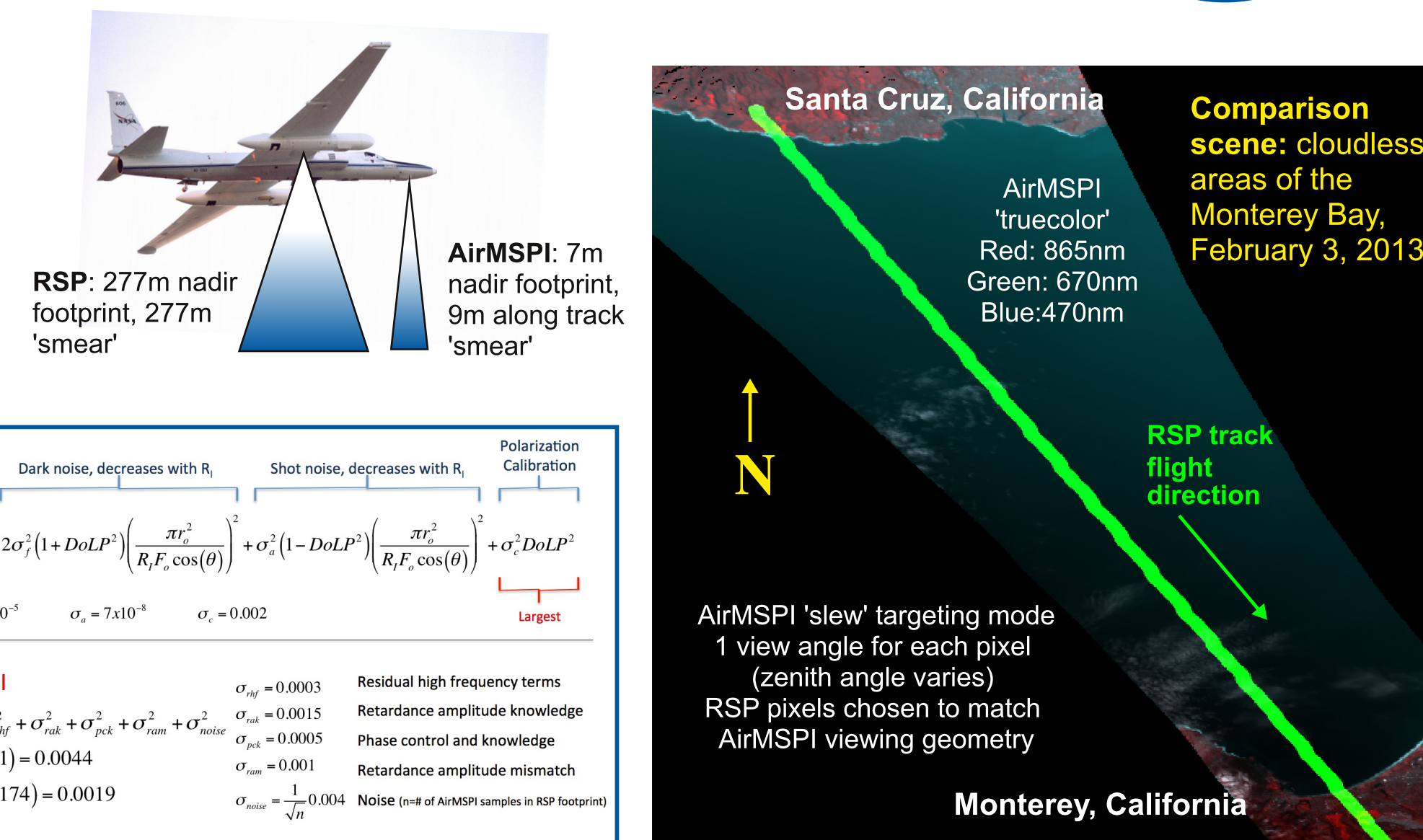
Type	Approximate Polarimetric accuracy	# view angles	Nadir ground resolution for ER-2 altitude	Channel center wavelength (nm)														total # obs. per pixel						
				355	380	410	445	470	550	555	660	670	766	865	870	935	960		1593	1880	2263			
AirMSPi	Photoelastic modulation, imager	0.5%	varies, max 31	7m footprint, 9m along track 'smear'																				up to 434
PACS	Philips prisms + linear polarizers, imager	0.5% (?)	varies, max ~65	37m footprint, smear?																				up to 1170
RSP	Wollaston Prisms, not an imager	0.2%	~152	277m footprint, 277m along track 'smear'																				4104

References
Cairns, B., Russell, E. E., LaVeigne, J. D., and Tennant, P. M., 2003: Research scanning polarimeter and airborne usage for remote sensing of aerosols. *Proc. SPIE*, 5158, 33-44.
Chowdhary, J., Cairns, B., Waquet, F., Knobelspiesse, K., Ottaviani, M., Redemann, J., Travis, L., and Mishchenko, M., 2012: Sensitivity of multangle, multispectral polarimetric remote sensing over open oceans to water-leaving radiances: Analyses of RSP data acquired during the MILAGRO campaign. *Remote Sensing of Environment*, 118, 284-308.
Diner, D. J., Davis, A., Hancock, B., Gutt, G., Chipman, R.A., and Cairns, B., 2007: Dual-photoelastic-modulator-based polarimetric imaging concept for aerosol remote sensing. *Appl. Opt.*, 46 (35), 8428-8445.
Diner, D. J., Xu, F., Garay, M. J., Martonchik, J. V., Rheingans, B. E., Geier, S., Davis, A., Hancock, B. R., Jovanovic, V. M., Bull, M. A., Capraro, K., Chipman, R. A., and McClain, S. C., 2013: The Airborne Multiangle SpectroPolarimetric Imager (AirMSPi): a new tool for aerosol and cloud remote sensing. *Atmospheric Measurement Techniques*, 6 (8), 2007-2025.
Knobelspiesse, K., Cairns, B., Redemann, J., Bergstrom, R. W., and Stohl, A., 2011: Simultaneous retrieval of aerosol and cloud properties during the MILAGRO field campaign. *Atmospheric Chemistry and Physics*, 11, 6245-6263.
Knobelspiesse, K., Cairns, B., Mishchenko, M., Chowdhary, J., Tsigaridis, K., van Diedenhoven, B., Martin, W., Ottaviani, M., and Alexandrov, M., 2012: Analysis of fine-mode aerosol retrieval capabilities by different passive remote sensing instrument designs. *Opt. Express*, 20 (19), 21457-21464.

Acknowledgements
This work is funded by the Aerosol, Cloud and Ecosystem (ACE) Mission, courtesy Hal Maring and David O. Starr, NASA HQ. Polarimeter data were used with the support of instrument PI's David Diner (AirMSPi - JPL), Brian Cairns (RSP - NASA GISS) and J. Vanderlei Martins (PACS - UMBC). Flight path plots were created by Matteo Ottaviani.

How do observed total and polarized reflectances compare?

Polarimeter teams are busy analyzing data (see posters A21F-0111, A21F-0124, A21F-0125, and talks this afternoon A24E-03, A24E-04, A24E-05, A24E-06, A24E-07). Our goal is to compare observed total and polarized reflectances from coincident scenes in order to verify calibration and validate the input to parameter retrieval algorithms.



Radiometric and Polarimetric uncertainty:

$$\sigma_{R_i}^2 = 2\sigma_i^2 \left(\frac{\pi R_i^2}{F_o \cos(\theta)} \right)^2 + \sigma_a^2 \left(\frac{R_i \pi R_i^2}{F_o \cos(\theta)} \right)^2 + \sigma_c^2 R_i^2$$

Dark noise, Shot noise, Calibration

For RSP, Largest by several orders of magnitude

Same for AirMSPi and RSP, although n=174 for AirMSPi, n=1 for RSP to account for averaging of higher spatial resolution AirMSPi data

RSP

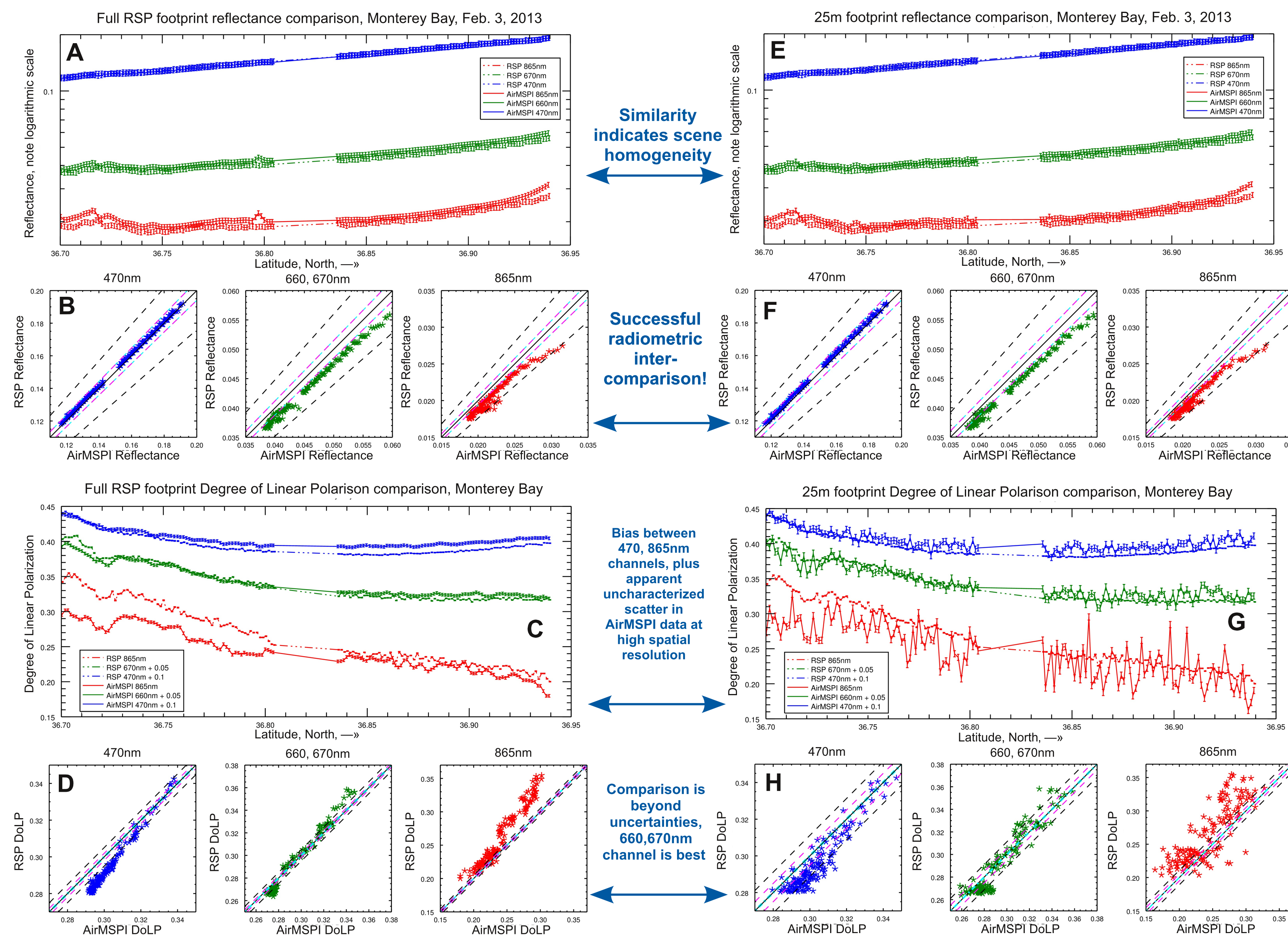
$$\sigma_{R_{tot}}^2 = 2\sigma_i^2 (1 + DoLP)^2 + \sigma_a^2 (1 - DoLP)^2 + \sigma_c^2 DoLP^2$$

$\sigma_i = 7 \times 10^{-3}$, $\sigma_a = 7 \times 10^{-4}$, $\sigma_c = 0.002$

AirMSPi

$\sigma_{R_{tot}}^2 = \sigma_{a,0}^2 + \sigma_{a,1}^2 + \sigma_{a,2}^2 + \sigma_{a,3}^2 + \sigma_{a,4}^2 + \sigma_{a,5}^2 + \sigma_{a,6}^2 + \sigma_{a,7}^2 + \sigma_{a,8}^2 + \sigma_{a,9}^2 + \sigma_{a,10}^2 + \sigma_{a,11}^2 + \sigma_{a,12}^2 + \sigma_{a,13}^2 + \sigma_{a,14}^2 + \sigma_{a,15}^2 + \sigma_{a,16}^2 + \sigma_{a,17}^2 + \sigma_{a,18}^2 + \sigma_{a,19}^2 + \sigma_{a,20}^2 + \sigma_{a,21}^2 + \sigma_{a,22}^2 + \sigma_{a,23}^2 + \sigma_{a,24}^2 + \sigma_{a,25}^2 + \sigma_{a,26}^2 + \sigma_{a,27}^2 + \sigma_{a,28}^2 + \sigma_{a,29}^2 + \sigma_{a,30}^2 + \sigma_{a,31}^2 + \sigma_{a,32}^2 + \sigma_{a,33}^2 + \sigma_{a,34}^2 + \sigma_{a,35}^2 + \sigma_{a,36}^2 + \sigma_{a,37}^2 + \sigma_{a,38}^2 + \sigma_{a,39}^2 + \sigma_{a,40}^2 + \sigma_{a,41}^2 + \sigma_{a,42}^2 + \sigma_{a,43}^2 + \sigma_{a,44}^2 + \sigma_{a,45}^2 + \sigma_{a,46}^2 + \sigma_{a,47}^2 + \sigma_{a,48}^2 + \sigma_{a,49}^2 + \sigma_{a,50}^2 + \sigma_{a,51}^2 + \sigma_{a,52}^2 + \sigma_{a,53}^2 + \sigma_{a,54}^2 + \sigma_{a,55}^2 + \sigma_{a,56}^2 + \sigma_{a,57}^2 + \sigma_{a,58}^2 + \sigma_{a,59}^2 + \sigma_{a,60}^2 + \sigma_{a,61}^2 + \sigma_{a,62}^2 + \sigma_{a,63}^2 + \sigma_{a,64}^2 + \sigma_{a,65}^2 + \sigma_{a,66}^2 + \sigma_{a,67}^2 + \sigma_{a,68}^2 + \sigma_{a,69}^2 + \sigma_{a,70}^2 + \sigma_{a,71}^2 + \sigma_{a,72}^2 + \sigma_{a,73}^2 + \sigma_{a,74}^2 + \sigma_{a,75}^2 + \sigma_{a,76}^2 + \sigma_{a,77}^2 + \sigma_{a,78}^2 + \sigma_{a,79}^2 + \sigma_{a,80}^2 + \sigma_{a,81}^2 + \sigma_{a,82}^2 + \sigma_{a,83}^2 + \sigma_{a,84}^2 + \sigma_{a,85}^2 + \sigma_{a,86}^2 + \sigma_{a,87}^2 + \sigma_{a,88}^2 + \sigma_{a,89}^2 + \sigma_{a,90}^2 + \sigma_{a,91}^2 + \sigma_{a,92}^2 + \sigma_{a,93}^2 + \sigma_{a,94}^2 + \sigma_{a,95}^2 + \sigma_{a,96}^2 + \sigma_{a,97}^2 + \sigma_{a,98}^2 + \sigma_{a,99}^2 + \sigma_{a,100}^2 + \sigma_{a,101}^2 + \sigma_{a,102}^2 + \sigma_{a,103}^2 + \sigma_{a,104}^2 + \sigma_{a,105}^2 + \sigma_{a,106}^2 + \sigma_{a,107}^2 + \sigma_{a,108}^2 + \sigma_{a,109}^2 + \sigma_{a,110}^2 + \sigma_{a,111}^2 + \sigma_{a,112}^2 + \sigma_{a,113}^2 + \sigma_{a,114}^2 + \sigma_{a,115}^2 + \sigma_{a,116}^2 + \sigma_{a,117}^2 + \sigma_{a,118}^2 + \sigma_{a,119}^2 + \sigma_{a,120}^2 + \sigma_{a,121}^2 + \sigma_{a,122}^2 + \sigma_{a,123}^2 + \sigma_{a,124}^2 + \sigma_{a,125}^2 + \sigma_{a,126}^2 + \sigma_{a,127}^2 + \sigma_{a,128}^2 + \sigma_{a,129}^2 + \sigma_{a,130}^2 + \sigma_{a,131}^2 + \sigma_{a,132}^2 + \sigma_{a,133}^2 + \sigma_{a,134}^2 + \sigma_{a,135}^2 + \sigma_{a,136}^2 + \sigma_{a,137}^2 + \sigma_{a,138}^2 + \sigma_{a,139}^2 + \sigma_{a,140}^2 + \sigma_{a,141}^2 + \sigma_{a,142}^2 + \sigma_{a,143}^2 + \sigma_{a,144}^2 + \sigma_{a,145}^2 + \sigma_{a,146}^2 + \sigma_{a,147}^2 + \sigma_{a,148}^2 + \sigma_{a,149}^2 + \sigma_{a,150}^2 + \sigma_{a,151}^2 + \sigma_{a,152}^2 + \sigma_{a,153}^2 + \sigma_{a,154}^2 + \sigma_{a,155}^2 + \sigma_{a,156}^2 + \sigma_{a,157}^2 + \sigma_{a,158}^2 + \sigma_{a,159}^2 + \sigma_{a,160}^2 + \sigma_{a,161}^2 + \sigma_{a,162}^2 + \sigma_{a,163}^2 + \sigma_{a,164}^2 + \sigma_{a,165}^2 + \sigma_{a,166}^2 + \sigma_{a,167}^2 + \sigma_{a,168}^2 + \sigma_{a,169}^2 + \sigma_{a,170}^2 + \sigma_{a,171}^2 + \sigma_{a,172}^2 + \sigma_{a,173}^2 + \sigma_{a,174}^2$

RSP reflectances and Degree of Linear Polarization (DoLP) compared to the mean value of the same for all AirMSPi observations within the same RSP footprint (left column) or a 25m subset or the RSP footprint (right column). DoLP is the ratio of polarized to total reflectance. Zenith and azimuth observation angles for the comparison match. AirMSPi uncertainty estimates due to random noise are reduced by 1/(n) according to the number of averaged pixels. **A,E:** South to North track of observed reflectances, individual error bars as defined above. **B,F:** Scatterplot comparisons. Black dashed lines are AirMSPi + RSP 2 sigma uncertainties, 95% should be within these bounds. **C,G:** Same as A,E for DoLP. **D,H:** Same as B,F for DoLP.



Conclusions

1. This analysis does NOT indicate which instrument is 'correct'.
2. AirMSPi and RSP reflectances agree within uncertainties. Comparisons of 25m to full footprint AirMSPi averages have no difference, indicating scene homogeneity.
3. Degree of Linear Polarizations do NOT agree within uncertainties:
 - There is a systematic bias between channels, although the 660,670nm comparison is nearly reasonable.
 - Higher spatial resolution AirMSPi data appears to have a random error that is uncharacterized. This is worst for 865nm. Ongoing efforts hope to identify the source of this uncertainty, and if it is present in different scene types.
4. Results call for unified polarimetric calibration techniques and cross-calibration efforts.
5. There is urgent need for full PACS and AirMSPi data availability.